

A Novel Approach for Automatic Palmprint Recognition

Murat Ekinici and Murat Aykut

Computer Vision Lab.
Department of Computer Engineering,
Karadeniz Technical University, Trabzon, Turkey
ekinici@ktu.edu.tr

Abstract. In this paper, we propose an efficient palmprint recognition scheme which has two features: 1) representation of palm images by two dimensional (2-D) wavelet subband coefficients and 2) recognition by a modular, personalized classification method based on Kernel Principal Component Analysis (Kernel PCA). Wavelet subband coefficients can effectively capture substantial palm features while keeping computational complexity low. We then kernel transforms to each possible training palm samples and then mapped the high-dimensional feature space back to input space. Weighted Euclidean linear distance based nearest neighbor classifier is finally employed for recognition. We carried out extensive experiments on PolyU Palmprint database includes 7752 palms from 386 different palms. Detailed comparisons with earlier published results are provided and our proposed method offers better recognition accuracy (99.654%).

1 Introduction

Biometrics is becoming more and more popular in an increasingly automated world. Palmprint recognition is one kind of biometric technology and a relatively new biometric feature. Compared with other biometrics, the palmprints has several advantages: low-resolution imaging can be employed; low-cost capture devices can be used; it is difficult to fake a palmprint; the line features of the palmprints are stable, etc. [1]. It is for these reasons that palmprint recognition has recently attracted an increasing amount of attention from researchers.

There are many approaches for palmprint recognition using line-based [2][4][5], texture-based [9][5], and appearance-based methods [3][8][7][6] in various literature. In the line-based approach, the features used such as principal lines, wrinkles, delta points, minutiae, etc. are sometimes difficult to extract directly from a given palmprint image with low resolution. The recognition rates and computational efficiency are not strong enough for palmprint recognition. In the texture-based approach, the texture features are not sufficient and the extracted features are greatly affected by the lighting conditions. From that disadvantages, researches have developed the appearance-based approaches. The appearance-based approaches only use a small quantity of samples in each palmprint class

randomly selected as training samples to extract the appearance features (commonly called algebraic features) of palmprints and form feature vector.

Eigenpalms method [8], fisherpalms method [3], and eigen-and-fisher palms [7] are presented as the appearance-based approaches for palmprint recognition in literature. Basically, their representations only encode second-order statistics, namely, the variance and the covariance. As these second order statistics provide only partial information on the statistics both natural images and palm images, it might become necessary to incorporate higher order statistics as well. In other words, they are not sensitive to higher order statistics of features. A kernel fisherpalm [6] is presented as another work to resolve that problem. In addition, for palmprint recognition, the pixelwise covariance among the pixels may not be sufficient for recognition. The appearance of a palm image is also severely affected by illumination conditions that hinder the automatic palmprint recognition process.

Converging evidence in neurophysiology and psychology is consistent with the notion that the visual system analyses input at several spatial resolution scales [19]. Thus, spatial frequency preprocessing of palms is justified by what is known about early visual processing. By spatial frequency analysis, an image is represented as a weighted combination of basis functions, in which high frequencies carry finely detailed information and low frequencies carry coarse, shape-based information. Recently, there have been renewed interests in applying discrete transform techniques to solve some problems in face recognition [13][14][17], in palmprint recognition [17][18] and many real world problems. An appropriate wavelet transform can result in robust representations with regard to lighting changes and be capable of capturing substantial palm features while keeping computational complexity low.

From these all considerations, we propose to use discrete wavelet transform (DWT) to decompose palm images and choose the lowest resolution subband coefficients for palm representation. We then apply kernel PCA as a nonlinear method to project palmprints from the high-dimensional palmprint space to a significantly lower-dimensional feature space, in which the palmprints from the different palms can be discriminated much more efficiently. The main contributions and novelties of the current paper are summarized as follows:

- To reliably extract palmprint representation, we adopt a template matching approach where the feature vector of a palm image is obtained through a multilevel two-dimensional discrete wavelet transform (DWT). The dimensionality of a palm image is greatly reduced to produce the *waveletpalm*.
- A nonlinear machine learning method, kernel PCA, is applied to extract palmprint features from the *waveletpalm*.
- The proposed algorithm is tested on a public palmprint databases. We provide some quantitative comparative experiments to examine the performance of the proposed algorithm and different combinations of the proposed algorithm. Comparison between the proposed algorithm and other recent approaches is also given.

This paper is organized as follows. Section 2 introduces briefly wavelet transform, lowest subband image representation, and fast Fourier transform (FFT) which is also implemented in this work to compare the efficiencies on the palmprint recognition. A brief description of kernel PCA (KPCA) and similarity measurement used are given in Sections 3 and 4 respectively. Experimental results on the palmprint database are summarized in Section 5 followed by discussions and conclusions in Section 6.

2 Discrete Transforms

In the proposed algorithm, the palmprint is first transformed into the wavelet domain, then kernel PCA is applied to extract higher order relations among waveletpalms for future recognition. In order to compare the efficiencies of the wavelet transform and discrete fast Fourier transform (FFT) is alternately employed in the proposed algorithm.

2.1 Discrete Wavelet Transform

The DWT was applied for different applications given in the literature e.g. texture classification [12], image compression, face recognition [13][14], because of its powerful capability for multiresolution decomposition analysis. The wavelet transform breaks an image down into four subsampled, or decimated, images. They are subsampled by keeping every other pixel. The results consist of one image that has been high pass filtered in both the horizontal and vertical directions, one that has been high pass filtered in the vertical and low pass filtered in the horizontal, one that has been lowpassed in the vertical and highpassed in the horizontal, and one that has been low pass filtered in both directions.

So, the wavelet transform is created by passing the image through a series of 2D filter bank stages. One stage is shown in Fig. 1, in which an image is first filtered in the horizontal direction. The filtered outputs are then down sampled by a factor of 2 in the horizontal direction. These signals are then each filtered by an identical filter pair in the vertical direction. Decomposed image into 4 subbands is also shown in Fig. 1. Here, H and L represent the high pass and low pass filters, respectively, and $\downarrow 2$ denotes the subsampling by 2. Second-level decomposition can then be conducted on the LL subband. Second-level structure of wavelet decomposition of an image is also shown in Fig. 1. This decomposition can be repeated for n-levels. Fig. 2 shows one-level, two-level and three-level wavelet decomposition of a palm image.

The proposed work based DWT addresses the four-level decomposition of images in the database used for experiments. Daubechies-8 [11] low pass and high pass filters are also implemented. Additionally, four-level of decompositions are produced, then 32 x 32 sub-images of 128 x 128 images in the wavelet are processed as useful features in the palmprint images. Reduce of the image resolution helps to decrease the computation load of the feature extraction process.

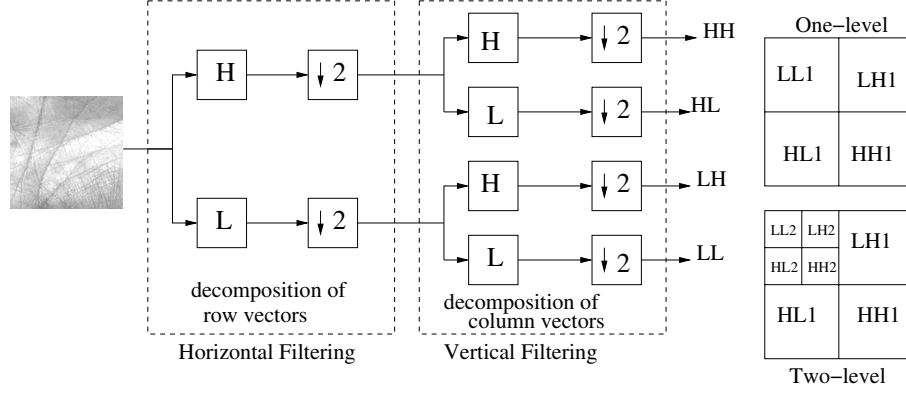


Fig. 1. One-level 2-D filter bank for wavelet decomposition and multi-resolution structure of wavelet decomposition of an image

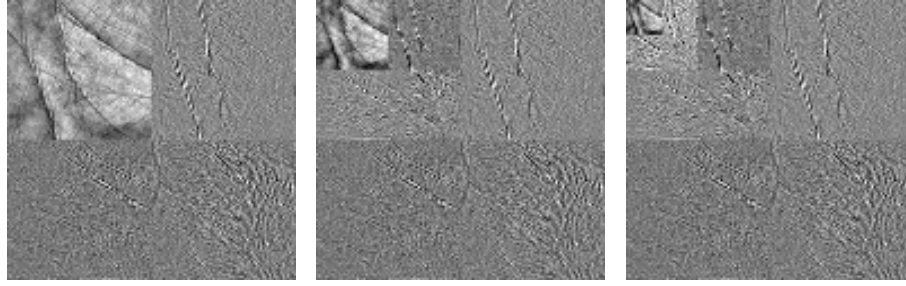


Fig. 2. Palm images with one-level, two-level, and three-level wavelet decomposition are shown

2.2 2-D Discrete FFT

$F(u, v)$ is 2-D FFT coefficients of $W \times H$ image $I(x, y)$. The feature sequence is generated using the 2D-FFT technique. The palmprint image (128×128) in the spatial domain is not divided into any overlap blocks. The FFT coefficients for the palmprint image are first computed. In FFT, the coefficients correspond to the lower frequencies than 3×3 , and to the higher frequencies than 16×16 in FFT, were discarded by filtering. In other words, 247 coefficients ($((16 \times 16) - (3 \times 3))$) correspond to the 6% coefficients in the frequency domain, (64×64) , were only processed. These data are empirically determined to achieve the best performance. Therefore, the size of the palmprint image (128×128) in the spatial domain was reduced to the very few coefficients in the frequency domain correspond to the 1.5% coefficient. Finally, $N = \mu x \nu$ features form a vector $\chi \in \mathbb{R}^N$, $\chi = (F_{0,0}, F_{0,1}, \dots, F_{\mu,\nu})$ for FFT.

3 Kernel PCA

The kernel PCA (KPCA) is a technique for nonlinear dimension reduction of data with an underlying nonlinear spatial structure. A key insight behind KPCA is to transform the input data into a higher-dimensional **feature space** [10]. The feature space is constructed such that a nonlinear operation can be applied in the input space by applying a linear operation in the feature space. Consequently, standard PCA can be applied in feature space to perform nonlinear PCA in the input space.

Let $\chi_1, \chi_2, \dots, \chi_M \in \mathbb{R}^N$ be the data in the input space (the input space is 2D-DWT coefficients in this work), and let Φ be a nonlinear mapping between the input space and the feature space i.e. using a map $\Phi : \mathbb{R}^N \rightarrow F$, and then performing a linear PCA in F . Note that, for kernel PCA, the nonlinear mapping, Φ , usually defines a kernel function [10]. The most often used kernel functions are polynomial kernels, Gaussian kernels, and sigmoid kernels [10]:

$$k(\chi_i, \chi_j) = \langle \chi_i, \chi_j \rangle^d, \quad (1)$$

$$k(\chi_i, \chi_j) = \exp\left(-\frac{\|\chi_i - \chi_j\|^2}{2\sigma^2}\right), \quad (2)$$

$$k(\chi_i, \chi_j) = \tanh(\kappa \langle \chi_i, \chi_j \rangle + \vartheta), \quad (3)$$

where d is a number in the set of natural numbers, e.g. $\{1, 2, \dots\}$, $\sigma > 0$, $\kappa > 0$, and $\vartheta < 0$.

The mapped data is centered, i.e. $\sum_{i=1}^M \Phi(\chi_i) = 0$ (for details see [10]), and let D represents the data matrix in the feature space: $D = [\Phi(\chi_1)\Phi(\chi_2) \dots \Phi(\chi_M)]$. Let $K \in \mathbb{R}^{M \times M}$ define a kernel matrix by means of dot product in the feature space:

$$K_{ij} = (\Phi(\chi_i) \cdot \Phi(\chi_j)). \quad (4)$$

The work in [10] shows that the eigenvalues, $\lambda_1, \lambda_2, \dots, \lambda_M$, and the eigenvectors, V_1, V_2, \dots, V_M , of kernel PCA can be derived by solving the following eigenvalue equation:

$$KA = MA\Lambda \quad (5)$$

with $A = [\alpha_1, \alpha_2, \dots, \alpha_M]$ and $\Lambda = \text{diag}\{\lambda_1, \lambda_2, \dots, \lambda_M\}$. A is MXM orthogonal eigenvector matrix, Λ is a diagonal eigenvalue matrix with diagonal elements in decreasing order ($\lambda_1 \geq \lambda_2 \geq \dots \geq \lambda_M$), and M is a constant corresponds to the number of training samples. Since the eigenvalue equation is solved for α 's instead of eigenvectors, $V = [V_1, V_2 \dots V_M]$, of kernel PCA, first, A should be normalized to ensure that eigenvalues of kernel PCA have unit norm in the feature space, therefore $\lambda_i \|\alpha_i\|^2 = 1, i = 1, 2, \dots, M$. After normalization the eigenvector matrix, V , of kernel PCA is then computed as follows:

$$V = DA \quad (6)$$

Now let χ be a test sample whose map in the higher dimensional feature space is $\Phi(\chi)$. The kernel PCA features of χ are derived as follows:

$$F = V^T \Phi(\chi) = A^T B \quad (7)$$

where $B = [\Phi(\chi_1) \cdot \Phi(\chi)\Phi(\chi_2) \cdot \Phi(\chi) \dots \Phi(\chi_M)\Phi(\chi)]^T$.

4 Similarity Measurement

When a palm image is presented to the wavelet-based kernel PCA classifier, the wavelet feature of the image is first calculated as detailed in Section 2, and the low-dimensional wavelet-based kernel PCA features, F , are derived using the equation 7. Let $M_k^0, k = 1, 2, \dots, L$, be the mean of the training samples for class w_k . The classifier applies, then, the nearest neighbor rule for classification using some similarity (distance) measure δ :

$$\delta(F, M_k^0) = \min_j \delta(F, M_j^0) \longrightarrow F \in w_k, \quad (8)$$

The wavelet-based kernel PCA feature vector, F , is classified as belong to the class of the closest mean, M_k^0 , using the similarity measure δ .

Popular similarity measures include the Weighted Euclidean Distance (WED) and Linear Euclidean Distance (LED) which are defined as follows:

$$WED : d_k = \sum_{i=1}^N \frac{(f(i) - f_k(i))^2}{(s_k)^2} \quad (9)$$

where f is the feature vector of the unknown palmprint, f_k and s_k denote the k th feature vector and its standard deviation, and N is the feature length.

$$LED : d_{ij}(\mathbf{x}) = d_i(\mathbf{x}) - d_j(\mathbf{x}) = 0 \quad (10)$$

where $d_{i,j}$ is the decision boundary separating class w_i from w_j . Thus $d_{ij} > 0$ for pattern of class w_i and $d_{ij} < 0$ for patterns of class w_j .

$$d_j(\mathbf{x}) = \mathbf{x}^T \mathbf{m}_j - \frac{1}{2} \mathbf{m}_j^T \mathbf{m}_j, \quad j = 1, 2, \dots, M \quad (11)$$

$$\mathbf{m}_j = \frac{1}{N_j} \sum_{\mathbf{x} \in w_j} \mathbf{x}, \quad j = 1, 2, \dots, M \quad (12)$$

where M is the number of pattern classes, N_j is the number of pattern vectors from class w_j and the summation is taken over these vectors.

Support Vector Machines (SVMs) have recently been known to be successful in a wide variety of applications [10][15]. SVM-based and WED-based classifier are also compared in this work. In SVM, we first have a training data set, like, $D = \{(x_i, y_i) | x_i \in X, y_i \in Y, i = 1, \dots, m\}$. Where X is a vector space of dimension d and $Y = \{+1, -1\}$. The basic idea of SVM consists in first mapping x into a high dimension space via a function, then maximizing the margin around the separating hyperplane between two classes, which can be formulated as the following convex quadratic programming problem:

$$\text{maximize} \quad W(\alpha) = \sum_{i=1}^m \alpha_i - \frac{1}{2} \sum_{i,j=1}^m \alpha_i \alpha_j y_i y_j (K(x_i, x_j) + \frac{1}{C} \delta_{i,j}) \quad (13)$$

$$\text{subject to} \quad 0 \leq \alpha_i \leq C, \forall_i, \quad (14)$$

$$\text{and} \quad \sum_i^m y_i \alpha_i = 0 \quad (15)$$

where $\alpha_i (\geq 0)$ are Lagrange multipliers. C is a parameter that assigns penalty cost to misclassification of samples. $\delta_{i,j}$ is the Kronecker symbol and $K(x_i, x_j) = \langle \phi(x_i) \cdot \phi(x_j) \rangle$ is the Gram matrix of the training examples. The form of decision function can be described as

$$f(x) = \langle w, \Phi(x) \rangle + b \quad (16)$$

where, $w = \sum_{i=1}^m \alpha_j^* y_i \Phi(x_i)$, and b is a bias term.

5 Experiments

The PolyU palmprint database [9] was obtained by collecting palmprint images from 193 individuals using a palmprint capture device. People was asked to provide about 10 images, each of the left and right palm. Therefore, each person provided around 40 images, so that this PolyU database contained a total of 7,752 grayscale images from 386 different palms. The samples were collected in two sessions, where the first ten samples were captured in the first session and other ten in the second session. The average interval between the first and second collection was 69 days. The resolution of all original palmprint images is 384 x 284 pixels at 75 dpi. In addition, they changed the light source and adjusted the focus of the CCD camera so that the images collected on the first and second occasions could be regarded as being captured by two different palmprint devices. The palmprint images collected in the second occasion were also captured under different lighting conditions.

At the experiments on the database, we use the preprocessing technique described in [9] to align the palmprints. In this technique, the tangent of the two holes (they are between the forefinger and the middle finger, and between the ring finger and the little finger) are computed and used to align the palmprint. The central part of the image, which is 128 x 128, is then cropped to represent the whole palmprint. Such preprocessing greatly reduces the translation and

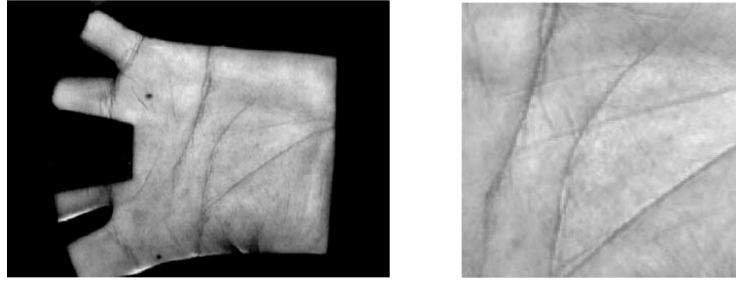


Fig. 3. Original palmprint and its cropped image

rotation of the palmprints captured from the same palms. An example of the palmprint and its cropped image is shown in Figure 3.

In the first experiment on the database, the first session was used as training set, second session includes 3850 samples of 386 different palms was also used as testing set. In this experiment, the features are extracted by using the proposed kernel based eigenspace method with length 50, 75, 100, 200, and 300. Weighted Euclidean distance(WED)-based matching was used to cluster those features. The matching is separately conducted and the results are listed in Table 1. The numbers given in Table 1 correspond to the correct recognition samples in all test samples (3850). The entries in brackets also represent the corresponding recognition rate. High recognition rate **93.168%** was achieved for the DWT+KPCA with feature length of 300. A nearest-neighbor classifier based on WED is employed to produce recognition rates given in the Table 1. The recognition rates obtained by PCA and kernel PCA based methods are comparatively illustrated in Table 1. When the feature number varies from 50 to 300, although KPCA-based approach only achieves higher recognition rate than PCA-based with feature length of 75, but DWT+KPCA based the proposed method achieved higher recognition rate then all combinations of PCA-based and FFT+KPCA-based approaches. Finally, it is evident that feature length can play an important role in the matching process. Long feature lengths lead to a high recognition rate.

Table 1. Comparative performance evaluation for the different matching schemes with different feature lengths. Train is first session, test is second session.

Method	Feature length				
	50	75	100	200	300
PCA	3411 (88.597)	3477 (90.311)	3498 (90.857)	3513 (91.246)	3513 (91.246)
DWT+PCA	3444 (89.454)	3513 (91.246)	3546 (92.103)	3570 (92.727)	3568 (92.675)
KPCA	3411 (88.597)	3481 (90.415)	3498 (90.857)	3508 (91.116)	3510 (91.168)
FFT+KPCA	2746 (71.324)	2933 (76.181)	3034 (78.805)	3174 (82.441)	3253 (84.493)
DWT+KPCA	3457 (89.792)	3531 (91.714)	3558 (92.415)	3584 (93.09)	3587 (93.168)

The performance variation for WED-based nearest-neighbor (NN) and SVM classifiers with the increase in number of features are shown in Figure 4. The SVM using radial basis function was employed in the experiments and the parameters of SVM were empirically selected. The training parameter γ , ϵ and C were empirically fixed at 0.55, 0.001, and 100, respectively. As shown in Figure 4, the SVM classifier achieved higher recognition when 50 features were only implemented. For the feature lengths longer than 50, the WED-based NN classifier has achieved better performance.

As final experiment and very similar to the experiments published in literature, the palm images collected from the first session were only used to test the proposed algorithm. We use the first four palmprint images of each person as training samples and the remaining six palmprint images as the test samples. So, the numbers of training and test samples are 1544 and 2316. We also test the

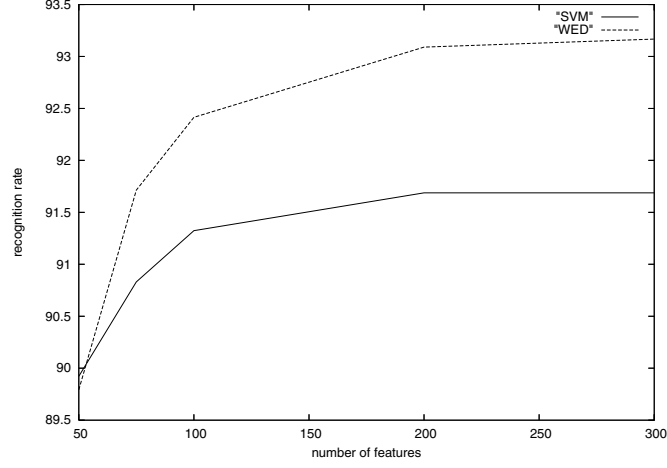


Fig. 4. Performance analysis of classifier with the number of features: DWT+ KPCA method using the SVM- and WED-based classifiers

Table 2. Testing results of the eight matching schemes with different feature lengths

Method		Feature length				
		50	100	200	300	380
PCA	LED	60.664 %	71.804 %	74.568 %	1723 (74.395 %)	1717 (74.136 %)
	WED	98.747 %	99.179 %	99.093 %	2294 (99.05 %)	2292 (98.963 %)
DWT + PCA	LED	59.542 %	71.459 %	87.305 %	2032 (87.737 %)	2032 (87.737 %)
	WED	98.834 %	99.309 %	99.352 %	2301 (99.352 %)	2302 (99.395 %)
KPCA	LED	63.557 %	73.661 %	75.82 %	1730 (74.697 %)	1712 (73.92 %)
	WED	98.877 %	99.222 %	99.05 %	2293 (99.006 %)	2291 (98.92 %)
DWT KPCA	LED	83.462 %	86.01 %	86.01 %	2025 (87.435 %)	2039 (88.039 %)
	WED	98.747 %	99.309 %	99.568 %	2308 (99.654 %)	2308 (99.654 %)

8 approaches against conventional PCA method using different test strategies. Based on these schemes, the matching is separately conducted and the results are listed in Table 2. The meaning of LED and WED in Table 2 is linear Euclidean discriminant and weighted Euclidean distance based nearest neighbor classifier, respectively. The numbers given for feature lengths 300 and 380 in Table 2 represent the number of the correct recognition samples in all 2316 palms used as test samples. The entries in the brackets also represent the corresponding recognition rate (%). A high recognition rate (**99.654 %**) was achieved for kernel PCA with 2D-DWT (abbreviated as DWT+KPCA) and WED classifier approach, with feature length of 300. One of the important conclusion from Table 2 is that, long feature lengths lead to a high recognition rate. However, this principle only holds to a certain point, as the experimental results summarized in Table 2 show that the recognition rate remain unchanged, or even become worse, when the feature length is extended further.

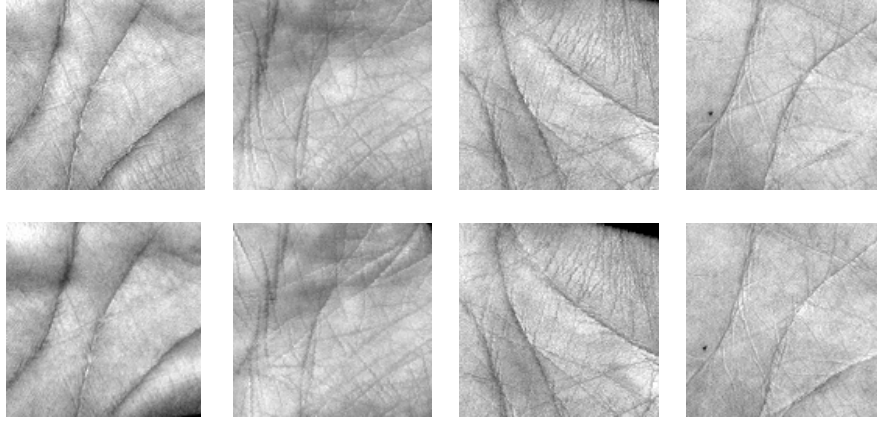


Fig. 5. Experimental results by the different rotation and translation conditions. (Top) Some palm images in training set, (Bottom) Correctly classified corresponding samples in testing set.

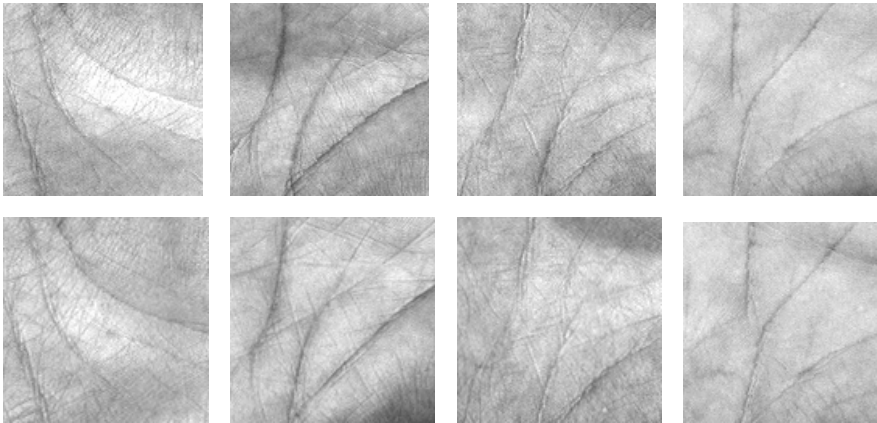


Fig. 6. Misclassified four palm samples. Top: Some palm images in training set, Bottom: Corresponding and misclassified samples in testing set.

Typical samples in this database are shown in Figs. 5 in which the top images were used as training samples, the bottom images were also used as test samples. Although the rotation and translation conditions are quite different from the samples used as test set, the proposed algorithm can still easily recognize the same palm. The misclassified samples were only 8 samples in all 2316 used as testing set, and some of them are also shown in Figure 6 in which the top images show the sample in training set, and corresponding bottom images were misclassified samples used in test set. The other misclassified four samples have not been shown because of the page limitation.

Table 3. Comparison of different palmprint recognition methods

	Method									
	Proposed	In [4]	In [5]	In [3]	In [8]	In [6]	In [7]	In [16]	In [17]	In [18]
Database palms	386	3	100	300	382	160	100	100	190	50
Database samples	3860	30	200	3000	3056	1600	600	1000	3040	200
Recog. Rate	99.654	95	91	99.2	99.149	97.25	97.5	95.8	98.13	98

Comparison has been finally conducted among our method and other methods published in literature, and is illustrated in Table 3. The databases given in the Table 3 are defined as the numbers of the different palms and whole samples tested. The data represent the recognition rates given in Table 3 is taken from experimental results in the cited papers. In biometric systems, the recognition accuracy will decrease dramatically when the number of image classes increase [1]. Although the proposed method is tested on the public database includes more different palms and samples, the recognition rate of our method is more efficient, as illustrated in Table 3.

6 Conclusion

This paper presents a new appearance-based non-linear feature extraction (kernel PCA) approach to palmprint identification that uses low-resolution images. We first transform the palmprints into wavelet domain to decompose the original palm images. The kernel PCA method is then used to project the palmprint image from the very high-dimensional space to a significantly lower-dimensional feature space, in which the palmprints from the different palms can be discriminated much more efficiently. WED based NN classifier is finally used for matching. The feasibility of the wavelet-based kernel PCA method has been successfully tested on PolyU database. The data set consists of 7752 images of 386 subjects. Experimental results show the effectiveness of the proposed algorithm for palmprint recognition.

Acknowledgments. This research is partially supported by The Research Foundation of Karadeniz Technical University (Grant No: KTU-2004.112.009.001). The authors would like to thank to Dr. David Zhang from the Hong Kong Polytechnic University, Hung Hom, Hong Kong, for providing us with the PolyU palmprint database.

References

1. Zhan D., Jing X., Yang J.: Biometric Image Discrimination Technologies. Computational Intelligence and Its Application Series, Idea Group Publishing, (2006) 80–95
2. Zhang D., Shu W.: Two Novel Characteristics in Palmprint Verification: Datum Point Invariance and Line Feature Matching. Pattern Recognition, Vol. 32, (1999) 691–702

3. Wu X., Zhang D., Wang K.: Fisherpalms Based Palmprint Recognition. *Pattern Recognition Letters*, Vol. 24, Issue 15, November, (2003) 2829–2838.
4. Duta N., Jain A.K., Mardia K.V.: Matching of Palmprint. *Pattern Recognition Letters*, Vol. 23, No.4, (2002) 477–485
5. You J., Li W., Zhang D.: Hierarchical Palmprint Identification via Multiple Feature Extraction. *Pattern Recognition*, Vol. 35 No.4, (2002) 847–859
6. Wang Y., Ruan Q., Kernel Fisher Discriminant Analysis for Palmprint Recognition. *IEEE The 18th Int. Conf. on Pattern Recognition, ICPR'06*, (2006) 457–460
7. Jiang W., Tao J., Wang L.: A Novel Palmprint Recognition Algorithm Based on PCA and FLD. *IEEE, Int. Conf. on Digital Telecommunications*, August, (2006) 28–32
8. Lu G., Zhang D., Wang K.: Palmprint Recognition Using Eigenpalms Features. *Pattern Recognition Letters*, Vol. 24, Issue 9-10, June (2003) 1463–1467
9. Zhang D., Kong W., You J., Wong M.: Online Palmprint Identification. *IEEE Trans. on Pattern Analysis and Machine Intelligence*, Vol. 25, No.9, September (2003) 1041–1049
10. Scholkopf B., Somala A.: *Learning with Kernel: Support Vector Machine, Regularization, Optimization and Beyond*. MIT Press, (2002).
11. Daubechies I.: *Ten Lectures on Wavelets*. Philadelphia, PA: SIAM, (1992).
12. Chang T., Kuo C.J.: Texture Analysis and Classification with Tree-Structured Wavelet Transform. *IEEE Trans. Image Processing*, Vol.2, No.4, (1993) 429–441
13. Zhang B., Zhang H., Sam S.: Face Recognition by Applying Wavelet Subband Representation and Kernel Associative Memory. *IEEE Transactions on Neural Networks*, Vol. 15, No. 1, (2004) 166–177
14. Chien J., Wu C., Discriminant Waveletfaces and Nearest Feature Classifier for Face Recognition. *IEEE Transactions on Pattern Analysis and Machine Intelligence*, Vol. 24, No. 12, (2002) 1644–1649.
15. Li W., Gong W., Yang L., Chen W., Gu X.: Facial Feature Selection Based on SVMs by Regularized Risk Minimization. *IEEE, The 18th Conference on Pattern Recognition (ICPR'06)*, (2006) 540–543
16. Kumar A., Zhang D.: Personal Recognition Using Hand Shape and Texture. *IEEE Transactions on Image Processing*, Vol. 5, No. 8, (2006) 2454–2460
17. Jing X.Y., Zhang D.: A Face and Palmprint Recognition Approach Based on Discriminant DCT Feature Extraction. *IEEE Transactions on Systems, Man, and Cybernetics-Part B: Cybernetics*, Vol. 34, No. 6 (2004) 2405–2415
18. Zhang L., Zhang D.: Characterization of Palmprints by Wavelet Signatures via Directional Context Modeling. *IEEE Trans. on Systems, Man, and Cybernetics-Part B: Cybernetics*, Vol. 34, No. 3, (2004) 1335–1347
19. Valentin T.: *Face-space Models of Face Recognition*. In *Computational, Geometric, and Process Perspectives on Facial Cognition: Context and Challenges*, Hillsdale, NJ: Lawrence Erlbaum, (1999)